Electronic Supplementary Material (ESI) for Environmental Science: Water Research & Technology.
This journal is © The Royal Society of Chemistry 2021

Supplementary Information

Effects of Peracetic Acid on Aromatic Polyamide Nanofiltration Membranes: A Comparative Study with Chlorine

Mohsen Ghafari[1], Tashfia M. Mohona[1], Lei Su[1], Haiqing Lin[2], Desiree L. Plata[3], Boya Xiong[3,4*], Ning Dai[1*]

[1]Department of Civil, Structural and Environmental Engineering, University at Buffalo, The State University of New York, Buffalo, NY 14260

[2]Department of Chemical and Biological Engineering, University at Buffalo, The State University of New York, Buffalo, NY 14260

[3]Department of Civil and Environmental Engineering, Massachusetts Institute of Technology, Cambridge, MA 02139

[4]Department of Civil, Environmental and Geo- Engineering, University of Minnesota, Minneapolis, MN 55455

* Corresponding authors:

Ning Dai: Email: ningdai@buffalo.edu. Phone: 716-645-4015. Address: 231 Jarvis Hall, Buffalo, NY 14260, USA.

Boya Xiong: Email: bxiong@umn.edu. Address: 500 Pillsbury Dr. SE, Minneapolis, MN 55455, USA.

4 texts, 7 figures, 8 tables

Text S1. Chemicals

NaOCl (available chlorine 4-4.99%), PAA (32% PAA in dilute acetic acid (40-45%) containing <6% H_2O_2), and H_2O_2 (30% in H_2O) were purchased from Sigma-Aldrich. Text S2 describes the methods used to determine the oxidant concentrations in the PAA, H_2O_2, and NaOCl stock solutions. The mass ratio of PAA to H_2O_2 in the commercial PAA stock was determined to be 5.9:1. Glycerol (≥ 99.5%, Fisher Chemicals), ethylene glycol (EG, Alfa Aesar), and polyethylene glycol 200 (PEG 200, Alfa Aesar) were used in the testing of organic rejection of the membranes. Benzanilide (≥ 98%, Alfa Aesar) was used as a small molecular model to study polyamide reaction mechanism. NaCl, Na_2HPO_4, NaH_2PO_4, $FeSO_4.7H_2O_2$, and anhydrous $Na_2S_2O_3$ were purchased from Fisher Chemicals. Deionized water from a Milli-Q Integral Water Purification System was used for all aqueous solutions.

Commercial PAA products contain H_2O_2 and acetic acid to minimize the hydrolysis of PAA during storage. Typically, at least one of these two components is in excess to PAA. For wastewater application, because of the concern of acetic acid raising the biochemical oxygen demand in the treated water, most formulations have excess amount of H_2O_2 (e.g., 15% PAA, 23% H_2O_2, and 16% acetic acid).[1]

Text S2. Oxidant Quantification Methods

Determining PAA concentration in the stock solution using iodometric titration. A PAA solution was prepared by adding 25 µL commercial stock (~32 wt%) in 20 mL Milli-Q water (i.e., 800-fold dilution). Catalase (0.1 g/L) was added to quench the H_2O_2 30 s prior to titration. Glacial acetic acid (5 mL) and KI (1 g) were added to the solution and, a yellow color was developed, indicating the formation of iodine. Titration with sodium thiosulfate solution (N = 0.04 N) was performed away from direct sunlight until the yellow color disappeared. 1 mL of starch indicator solution (1%) was added, and a blue color was formed. The titration was continued until the blue color disappeared. The total volume of sodium thiosulfate titrant in this step was recorded as A. Blank titration was performed using Milli-Q water, the total volume of sodium thiosulfate titrant was recorded as B. PAA concentration was calculated using Equation S1. The commercial PAA stock concentration was then calculated after accounting for the 800-fold dilution:

$$PAA\ \left(\frac{mg}{L}\right) = \frac{(A-B)\times N\times 38.025\times 1000}{20\ (ml)} \quad \text{(Eq. S1)}$$

Measuring PAA residual concentrations in oxidant exposure experiments using DPD colorimetric method. After a pre-selected exposure period, the samples were diluted to achieve an estimated PAA concentration within the range of 0.2–2 mg L^{-1}. A Hach 25-mL TOTAL Chlorine powder pillow was added to 10 mL of a diluted sample in an Amber glass vial. The vial was shaken for 20 s, and the absorbance was measured after 1 min at 553 nm by a UV-Vis spectrophotometer (Agilent, Cary 60). The PAA concentration was calculated using a previously developed calibration curve.

Determining H_2O_2 concentration in the stock solution based on UV absorbance. A H_2O_2 solution was prepared by adding 25 µL commercial stock (~30 wt%) in 20 mL Milli-Q water. UV absorbance of the solution was measured at 254 nm. The H_2O_2 concentration was calculated using the H_2O_2 molar extinction coefficient (ε_{254}) of 18 M^{-1} cm^{-1} reported by Bolton and Cater.[2]

Measuring H_2O_2 residual concentrations in oxidant exposure experiments using DPD colorimetric method. After a pre-selected exposure period, the samples were diluted to achieve an estimated H_2O_2 concentration within the range of 0.2–2 mg L^{-1}. Three drops of 20 wt% KI solution and 3 drops of molybdate reagent (ammonium molybdate, Hach Company, CO, USA) were added to the 10 mL diluted sample. The vial was shaken for 20 s and set aside for 6 min. A Hach 25-mL TOTAL Chlorine powder pillow was then added to the solution, and the absorbance was measured at 553 nm, which indicates the sum of PAA and H_2O_2 molar concentrations. H_2O_2 concentration was calculated using a previously developed calibration curve. For samples containing both PAA and H_2O_2, the H_2O_2 concentration was obtained by subtracting the molar concentration of PAA from the total molar concentration of peroxides.

Determining chlorine concentration in the NaOCl stock solution based on UV absorbance. The commercial chlorine stock (4–5%) was diluted to achieve an estimated concentration of 100 mg L^{-1}. Absorbance was measured at 245 nm and 295 nm. The following equations were used to determine chlorine concentration in the stock solution.

$$A_{245nm} = \varepsilon_{[OCl^-]_{245nm}}[OCl^-] + \varepsilon_{[HOCl]_{245nm}}[HOCl] \quad \text{(Eq. S2)}$$

$$A_{295nm} = \varepsilon_{[OCl^-]_{295nm}}[OCl^-] + \varepsilon_{[HOCl]_{295nm}}[HOCl] \quad \text{(Eq. S3)}$$

where A_{245nm} and A_{295nm} are the sample absorbance at 245 and 295 nm, respectively; the molar extinction coefficients for OCl^- at 245 and 295 nm are 46 and 343 M^{-1} cm^{-1}, respectively, while those for HOCl are 105 and 40 M^{-1} cm^{-1}, respectively.

Measuring chlorine residual concentration using DPD colorimetric method. Similar to the previous method, samples were diluted to bring chlorine concentration below 2 mg L^{-1} in 10 mL Milli-Q water. A DPD 10-mL TOTAL Chlorine powder pillow was added to the solution in an Amber glass vial. The vial was shaken for 20 s and the absorbance was measured after 3 min at 515 nm using a UV-Vis spectrophotometer. The total chlorine concentration was determined using a previously developed calibration curve.

Text S3. Analysis of Benzanilide and Degradation Products

Benzanilide was analyzed by high-performance liquid chromatography with a diode array detector (HPLC-DAD, Agilent 1260 Infinity). An Agilent Poroshell 120 EC-C18 analytical column (4.6 mm × 100 mm, 2.7 μm) and its guard column ECC18 (4.6 mm × 5 mm, 2.7 μm) were used and maintained at 30 °C during analysis. Sample injection volume was 15 μL. Eluent flow rate was 1 mL min^{-1}; an isocratic elution with 45% 15 mM pH 2.6 phosphate buffer and 55% acetonitrile was used. The detection wavelength was 264 nm. The retention time for benzanilide was 2.3 min. The detection limit was 0.5 μM.

For the analysis of benzoic acid and the exploration of other benzanilide degradation products, a liquid chromatography triple quadrupole mass spectrometer (LC-QQQ, Agilent 6470) was used. An Agilent ZORBAX RRHD Eclipse Plus C18 analytical column (3 mm × 50 mm, 1.8 μm) and its guard column C18 (3 mm × 5 mm, 1.8 μm) were used and maintained at 30 °C during analysis. For benzoic acid analysis, the eluent flow rate was set at 0.2 mL min^{-1}, with isocratic elution using 30% water (with 0.1% formic acid) and 70% acetonitrile. The retention time of benzoic acid was 3.66 min. Sample injection volume was 15 μL. Electron spray ionization (ESI)

was operated in the positive mode. Fragmentor was set at 130; collision energy was 30 eV. The detection limit of benzoic acid was 0.01 μM. To explore other benzanilide degradation products, the eluent flow rate was set at 0.2 mL min^{-1}, with gradient elution: 5% acetonitrile and 95% water for the first 3 min, followed by a ramp from 3 to 15 min to reach 95% acetonitrile and 5% water, which is maintained for the next 5 min; the eluent composition was returned to 5% acetonitrile and 95% water in 1 min and maintained for another 2 min. In this gradient method, the retention time of benzanilide and benzoic acid was 14.38 and 11.64 min, respectively. Sample injection volume was 15 μL. Both positive and negative ESI were employed; results from the negative mode feature higher signal to noise ratio, and are reported in section 3.3.2.

Text S4. Effects of High Chloride Concentration on Polyamide Membrane Performance

Although wastewater-level chloride did not affect the performance of NF90 membrane upon exposure to PAA, higher chloride concentrations such as that encountered in seawater can cause detrimental effects (Figure S6). After being exposed to a solution of 100 mg/L PAA and 540 mM chloride for 24 h, the pure water flux of the membrane dropped to 6.0 L m^{-2} h^{-1}, more than 75% lower than that of the pristine membrane or the membrane exposed to 100 mg/L PAA alone. Additional membrane exposure experiments were conducted using solutions of NaCl (540 mM), PAA+Na_2SO_4 (540 mM), NaOCl (100 mg/L), or mixtures of NaOCl with NaCl (540 mM) at pH 5.5 and 6.5 (Figure S6). The comparison of the pure water fluxes of these membranes suggest that at high chloride concentrations, three factors may contribute to substantial polyamide membrane degradation: the formation of HOCl from the PAA-chloride reaction (reaction 2 in the main text), membrane deswelling due to high ionic strength (i.e., similar to Figure S2), and the favorable equilibrium towards the stronger chlorinating agent Cl_2 (reaction S1).[3]

$HOCl + Cl^- + H^+ = Cl_{2(aq)} + H_2O$ (reaction S1) $K_{eq} = 2.3 \times 10^3$

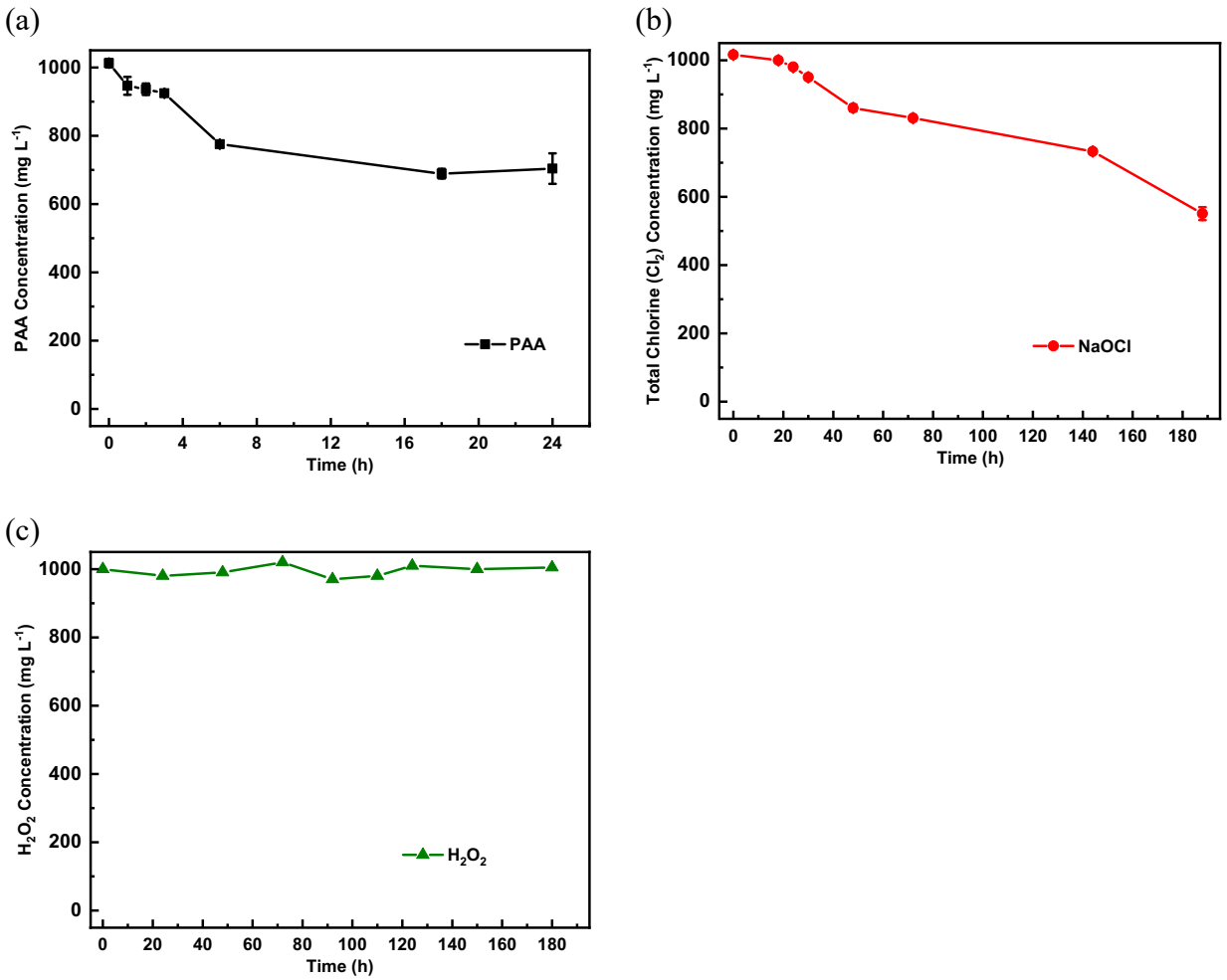

Figure S1. The concentration-time profiles of (a) PAA, (b) NaOCl, and (c) H_2O_2 in unbuffered Milli-Q water. Initial oxidant concentration 1000 mg L^{-1}, initial pH 6.5, room temperature.

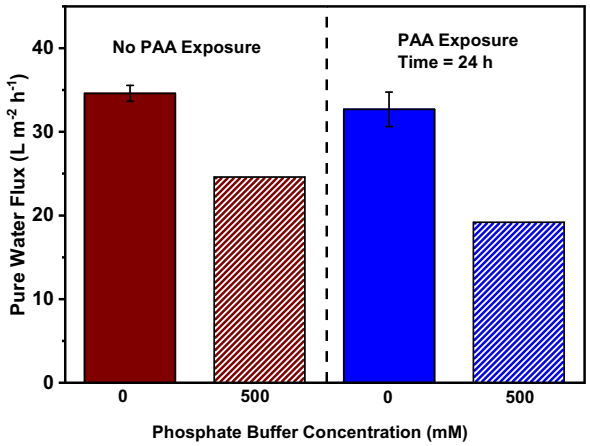

Figure S2. Effect of 24 h exposure to 500 mM phosphate buffer on membrane water flux. Initial pH 6.5, room temperature, initial PAA concentration 1000 mg L^{-1}. Pure water flux was tested at 4 bar. Even in the absence of PAA, exposure to 500 mM phosphate for 24 h resulted in substantial loss of membrane water permeability.

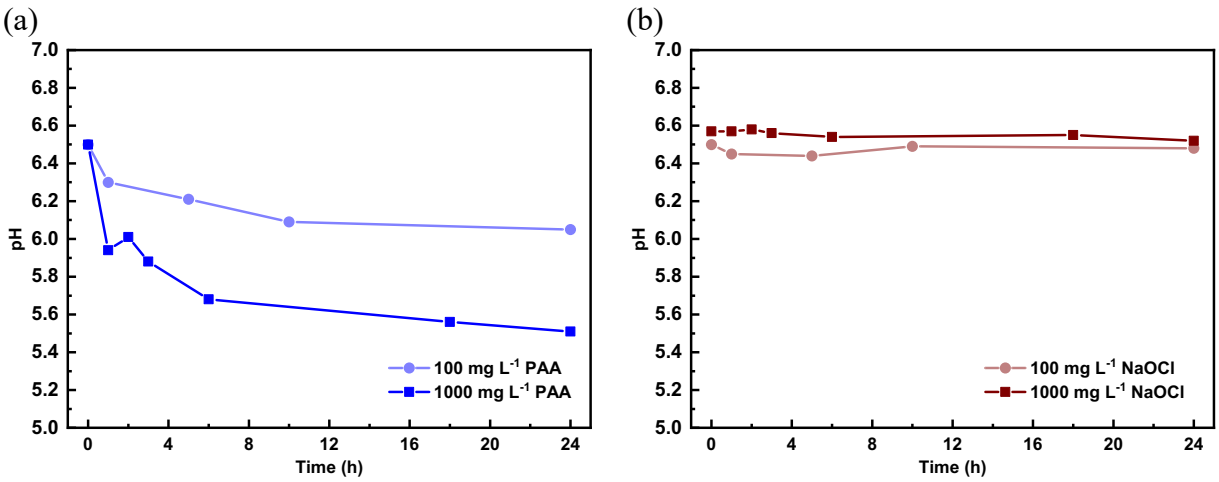

Figure S3. Change in oxidant solution pH over 24 h. Initial pH was adjusted to 6.5 by NaOH or HCl.

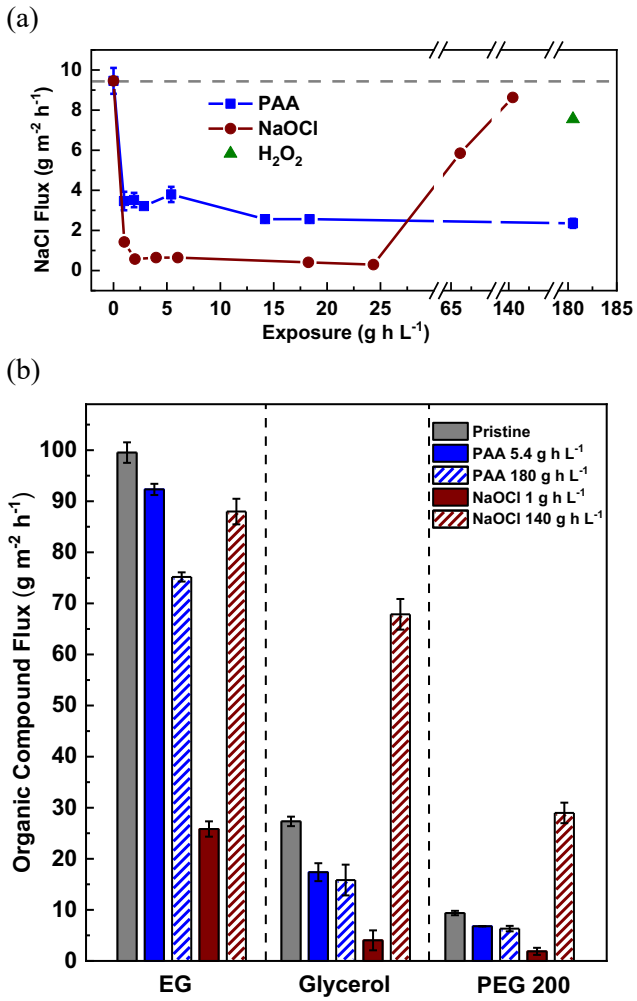

Figure S4. Change in the flux of (a) NaCl and (b) organic compounds upon oxidant exposure. The dash line in (a) represents the average value for the pristine membranes from duplicate tests. Experimental conditions are as described in the caption of Figure 1 and in sections 2.2 and 2.3.

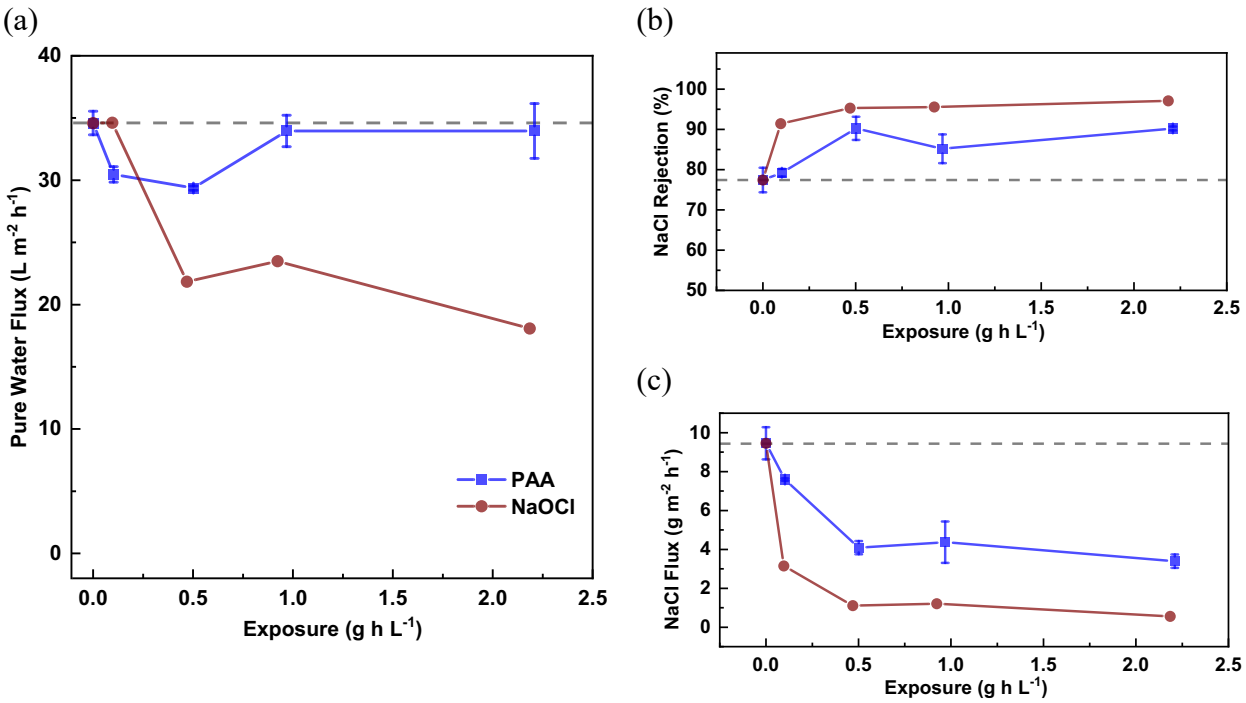

Figure S5. Comparison of (a) pure water flux, (b) NaCl rejection, and (c) NaCl flux among pristine and oxidant-exposed NF90 membranes. Initial oxidant concentration was 100 mg/L. All other test conditions are as described in the caption of Figure 1 and in sections 2.2 and 2.3. Selected PAA exposure experiments were conducted in duplicates, with error bars showing the difference between the two replicates. The dash line represents the average values for duplicate tests for the pristine membranes.

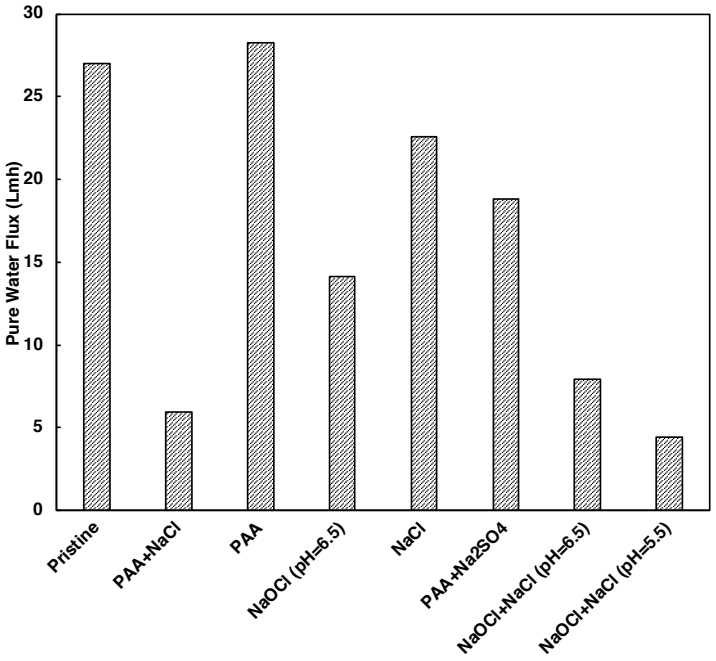

Figure S6. Effect of chloride on the pure water flux (L m $^{-2}$ h^{-1}) of NF90 membrane upon PAA or NaOCl exposure. NaCl or Na_2SO_4 concentration was 540 mM. PAA or NaOCl initial concentration 100 mg L^{-1}; exposure time 24 h. Other test conditions are as described in sections 2.2 and 2.3.

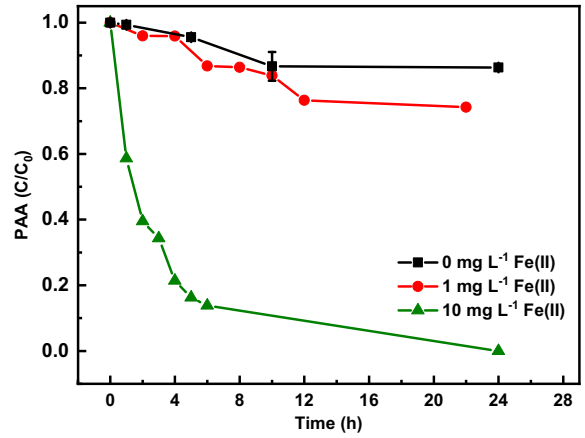

Figure S7. Time profiles of PAA decay in the presence of different concentrations of Fe(II). Initial PAA concentration was 100 mg L^{-1}; initial pH was adjusted to 6.5; room temperature.

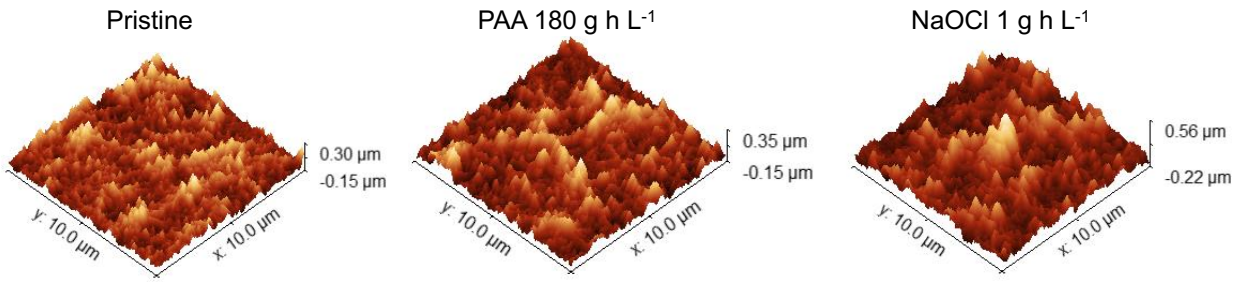

Figure S8. AFM images of pristine, PAA-exposed, and NaOCl-exposed membranes.

Table S1. Solution conditions for the first set of benzanilide degradation experiments. Experiment IDs match the legends in Figure 6a.

Experiment ID	PAA		H_2O_2		Fe(II)[a]	
	mg L^{-1}	mM	mg L^{-1}	mM	mg L^{-1}	µM
PAA	1,000	13.2	169[b]	5.0	0	0
H_2O_2	0	0	1,000	29	0	0
PAA+Fe	1,000	13.2	169	5.0	10	179
H_2O_2(1)+Fe	0	0	1,000	29	10	179
H_2O_2(2)+Fe	0	0	2,000	59	10	179
PAA+H_2O_2+Fe	1,000	13.2	2,169	64	10	179
Control	0	0	0	0	0	0

[a] Added as $FeSO_4$

[b] From Sigma-Aldrich PAA stock

Table S2. Solution conditions for the second set of benzanilide degradation experiments. Experiment IDs match the legends in Figure 6b.

Experiment ID	PAA		H_2O_2		Fe(II)[a]	
	mg L^{-1}	µM	mg L^{-1}	µM	mg L^{-1}	µM
PAA	7.6	100	1.3[b]	38	0	0
PAA+Fe	7.6	100	1.3	38	5.6	100
H_2O_2(1)+Fe	0	0	1.3	38	5.6	100
H_2O_2(2)+Fe	0	0	8.1	238	5.6	100
PAA+H_2O_2+Fe	7.6	100	8.1	238	5.6	100

[a] Added as $FeSO_4$

[b] From Sigma-Aldrich PAA stock

Table S3. PAA exposure to membranes in the presence of chloride or Fe(II).

Oxidant	Solution condition				PAA exposure (g h L^{-1})
	$[PAA]_0$ (mg L^{-1})	$[H_2O_2]_0$ (mg L^{-1})	[Fe(II)] (mg L^{-1})	$[Cl^-]$ (mg L^{-1})	
PAA	100	17	0	0	2.21
	100	17	0	300	1.89
	100	17	0	1200	1.66
	100	17	1	0	1.80
	100	17	10	0	0.29
PAA+H_2O_2	100	217	0	0	2.14
	100	217	0	300	1.10
	100	217	0	1200	0.94
	100	217	1	0	0.57
	100	217	10	0	0.12

Table S4. Time profile of benzanilide decay in the first set of degradation experiments.[a]

PAA			H_2O_2			PAA+Fe		
Time (h)	Benzanilide (μM)		Time (h)	Benzanilide (μM)		Time (h)	Benzanilide (μM)	
	Set 1	Set 2		Set 1	Set 2		Set 1	Set 2
0	30.4	27.3	0	29.7	38.7	0	30.1	27.6
50	24.8	24.4	50	28.1	37.8	50	29.6	24.5
75	24.4	23.7	75	26.1	33.8	75	20.8	20.2
120	18.2	13.6	100	21.6	27.7	120	12.8	17.1

H_2O_2(1)+Fe			H_2O_2(2)+Fe			PAA+H_2O_2+Fe		
Time (h)	Benzanilide (μM)		Time (h)	Benzanilide (μM)		Time (h)	Benzanilide (μM)	
	Set 1	Set 2		Set 1	Set 2		Set 1	Set 2
0	13.9	15.2	0	16.1	14.8	0	26.9	30.0
1.5	6.4	6.2	1.5	4.7	3.7	3	23.8	27.9
3	4.7	4.3	3	< 0.5	< 0.5	6	22.4	27.7
6	< 0.5	< 0.5				18	22.3	23.8
						42	4.5	3.4

Control		
Time (h)	Benzanilide (μM)	
	Set 1	Set 2
0	24.4	
1.5	23.4	
3	24.0	
6	24.2	
24	23.8	
31	24.4	
47	24.8	
83	24.7	

[a] Experiment IDs match those in Table S1 and Figure 6a. Experiments were conducted in duplicates except for Control.

Table S5. Time profile of benzanilide decay in the second set of degradation experiments.[a]

PAA		PAA+Fe		H_2O_2(1)+Fe		H_2O_2(2)+Fe		PAA+H_2O_2+Fe	
Time (h)	Conc. (μM)	Time (h)	Conc. (μM)	Time (h)	Conc. (μM)	Time (h)	Conc. (μM)	Time (h)	Conc. (μM)
0.00	25.9	0.00	24.2	0.08	23.2	0.08	13.9	0.00	21.0
2.48	28.3	0.13	24.4	0.17	21.9	0.17	10.8	0.17	13.1
25.10	28.5	2.67	24.3	0.25	20.8	0.42	9.9	2.68	10.2
		25.27	24.2	0.50	20.0	0.67	8.9	25.28	10.3
				0.92	19.6	1.22	9.0		
				1.88	19.5	2.23	8.9		
				2.32	19.0	3.33	8.1		
				3.32	19.9	6.28	8.2		
				3.43	19.6				
				6.38	19.8				

[a] Experiment IDs match those in Table S2 and Figure 6b.

Table S6. Pseudo first-order decay rate constants (k) of benzanilide in the first set of degradation experiments.[a]

Experiment ID	k (h^{-1})	Fitting r^2
PAA	$(4.1 \pm 0.67) \times 10^{-3}$	0.9265
H_2O_2	$(2.5 \pm 0.55) \times 10^{-3}$	0.8710
PAA+Fe	$(4.7 \pm 0.73) \times 10^{-3}$	0.9343
H_2O_2(1)+Fe	$(4.2 \pm 0.47) \times 10^{-1}$	0.9763
H_2O_2(2)+Fe	$(6.6 \pm 0.72) \times 10^{-1}$	0.9769
PAA+H_2O_2+Fe	$(4.1 \pm 0.64) \times 10^{-2}$	0.9103

[a] Experiment IDs match those in Table S1 and Figure 6a. Experiments were conducted in duplicates.

Table S7. Comparison of benzanilide decay and benzoic acid formation

pH	Sample	Reaction time (h)	ΔBenzanilide (μM)[a]	Benzoic acid (μM)	Percentage[b]
6.5	PAA	120	11.1	1.89	17%
	H_2O_2	120	9.6	0.28	2.9%
3[c]	PAA	120	12.9	0.64	4.9%
	H_2O_2	100	9.6	0.22	2.3%
	PAA+Fe	120	13.9	1.89	13.6%
	H_2O_2(1)+Fe	1.5	18.7	1.14	6.1%
	H_2O_2(2)+Fe	1.5	20.8	1.07	5.2%
	PAA+H_2O_2+Fe	3	24.6	0.43	1.8%

[a] ΔBenzanilide is the difference in benzanilide concentrations between the time zero sample and the sample analyzed after the reaction time specified in the table.
[b] The fraction of benzanilide decay that can be accounted for by benzoic acid formation.
[c] Reaction conditions are as described in Table S1.

Table S8. Oxidation products of benzanilide under different solution conditions

pH	Sample	Reaction time (h)	Product peaks with M/z = 212[a]		
			A1	A2	B
6.5	PAA	120	×	×	×
	H_2O_2	120	√	√	√
3[b]	PAA	120	√	√	√
	H_2O_2	100	√	×	√
	PAA+Fe	120	×	×	×
	H_2O_2(2)+Fe	1.5	?	?	?
	PAA+H_2O_2+Fe	3	?	?	?
Postulated structures			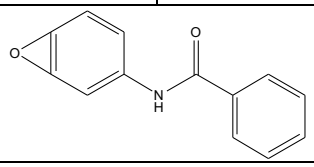		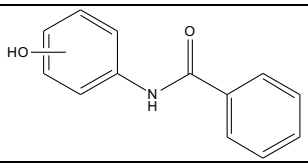

[a] Negative ionization mode. Product peaks A1 and A2 elute at 15.1 and 17.0 min, respectively. Product peak B elutes at 14.1 min. Products are considered present only if they are absent in the time zero samples. √ = present, × = absent, ? = inconclusive. Due to the fast kinetics in H_2O_2(2)+Fe and PAA+H_2O_2+Fe samples, reaction may have occurred in the time zero samples.
[b] Reaction conditions are as described in Table S1.

Reference:

1. Water Environment Association of Texas, Peracetic Acid for Disinfection of Municipal Wastewater Effluent, 2017. ftp.weat.org/Presentations/2017_Peracetic_Acid_Slides.pdf Accessed Oct. 1, 2020
2. J. R. Bolton and S. R. Cater, in *Aquatic and surface photochemistry*, CRC Press, 2018, pp. 467-490.
3. K. Huang, K. P. Reber, M. D. Toomey, H. Haflich, J. A. Howarter and A. D. Shah, Reactivity of the Polyamide Membrane Monomer with Free Chlorine: Reaction Kinetics, Mechanisms, and the Role of Chloride, *Environmental Science & Technology*, 2019, **53**, 8167-8176.